Proceedings of the ASME 2017 36th International Conference on Ocean, Offshore and Arctic Engineering
OMAE2017
June 25-20, 2017, Trondheim, Norway

OMAE2017-61804

AN EXPERIMENTAL AND NUMERICAL INVESTIGATION OF THE EFFECT OF AXIAL THERMAL GRADIENTS IN FLEXIBLE PIPES

Dag Fergestad
SINTEF Ocean [1]
Trondheim, Norway

Frank Klæbo
SINTEF Ocean [1]
Trondheim, Norway

Jan Muren
4Subsea
Asker, Norway

Pål Hylland
STATOIL
Stavanger, Norway

Tom Are Grøv
4Subsea
Asker, Norway

Hans Lange
SINTEF Materials and Chemistry
Trondheim, Norway

Janne K.Ø.Gjøsteen
SINTEF Ocean [1]
Trondheim, Norway

Andreas Gjendal
4Subsea
Asker, Norway

Bjørn Melve
STATOIL
Trondheim, Norway

Claus Egebjerg Kristensen
STATOIL
Oslo, Norway

ABSTRACT

This paper discusses the structural challenges associated with high axial temperature gradients and the corresponding internal cross section forces. A representative flexible pipe section designed for high operational temperature has been subject to full scale testing with temperature profiles obtained by external heating and cooling. The test is providing detailed insight in onset and magnitude of relative layer movements and layer forces. As part of the full-scale testing, novel methods for temperature gradient testing of unbonded flexible pipes have been developed, along with layer force- and deflection-measurement techniques. The full-scale test set-up has been subject to numerous temperature cycles of various magnitudes, gradients, absolute temperatures, as well as tension cycling to investigate possible couplings to dynamics.

Extensive use of finite element analysis has efficiently supported test planning, instrumentation and execution, as well as enabling increased understanding of the structural interaction within the unbonded flexible pipe cross section. When exploiting the problem by finite element analysis, key inputs will be correct material models for the polymeric layers, and as-built dimensions/thicknesses. Finding the balance between reasonable simplification and model complexity is also a challenge, where access to high quality full-scale tests and dissected pipes coming back from operation provides good support for these decisions.

Considering the extensive full scale testing, supported by advanced finite element analysis, it is evident that increased attention will be needed to document reliable operation in the most demanding high temperature flexible pipe applications.

INTRODUCTION

Increased production from high temperature reservoirs drives the demand for flexible riser and flowline systems capable of handling operational temperatures above 110-120 °C. In areas with topside hang-off in cold environment (water/air) or where subsea tie-in is in deep, cold waters, there may be a large difference between the highest bore temperature and the coldest external exposure.

During start-up and shut-down of high temperature unbonded flexible pipes, large axial temperature gradients may be experienced near the pipe ends. In applications where external protection, continuous buoyancy, bend restrictors or bend stiffeners are providing a high degree of insulation while the surrounding air or water is cold, the pipe wall temperature differences over a given length is found to be as high as 100°C. The temperature in the pipe wall will change axially and

[1] Earlier MARINTEK, SINTEF Ocean from January 1st 2017 through merger internally in the SINTEF Group

radially over time, as the pipe approaches a steady state operational or shut-in temperature. The differences in temperature expansion coefficients in the polymer and steel layers, along with temperature gradients, will inevitably create forces in the pipe wall layers, which may not be fully transferred to the tensile wires. It is noted that axial movement of inner layers are not covered by conventional design codes, and that conventional qualification testing only cover changes in temperatures that are constant over the length of the pipe and end fitting.

From experience with 1-layer PVDF pipe design, the Petroleum Company has initiated an investigation of the effect of axial thermal gradients in flexible pipes. As part of this investigation, a laboratory test of an 8 m long 9" ID pipe is carried out. The test focuses on the shut-down scenario and temperatures are imposed from the outside. For high temperature pipes, the maximum temperatures in outside insulating elements may be in the range of 100 °C to 110 °C, heated by the internal flow, whereas the outside low temperature from water or air may be in the range of 0 °C to -25 °C. During shut-down the internal heating stops, the insulating elements are still warm, and the bore is assumed fully depressurized at the time of the most critical axial thermal gradients. The lengths of applied temperature zones during testing is shown in Figure 1 for two different set-ups.

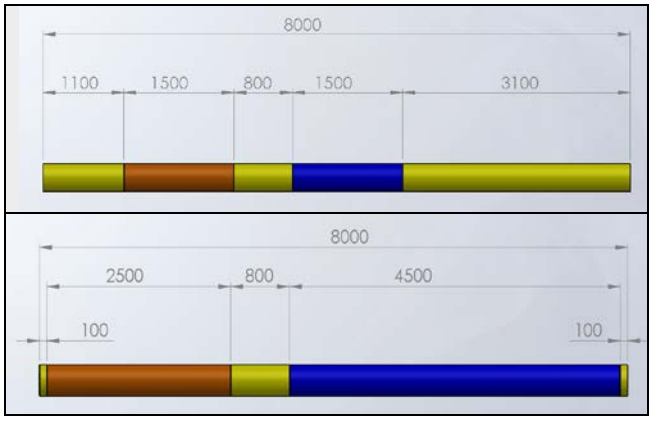

FIGURE 1. PIPE TEMPERATURE ZONES DURING TEMPERATURE GRADIENT BUILD-UP: WARM SECTION (RED), COLD SECTION (BLUE), GRADIENT SECTION (800 MM YELLOW MIDDLE SECTION). UPPER FIGURE USED FOR INITIAL TESTING (LC01-02), LOWER FIGURE USED FOR EXTENDED TESTING (LC03-05).

PRE-TEST ANALYSIS

The preparatory work for the test has been conducted in phases, including an initial pilot test of a 2.6 m long pipe sample and various smaller trials of monitoring equipment solutions. Thermal FE-analyses are performed in order to determine the temperature distributions, axially, radially and over time. This is for the control of externally heated and cooled zones to obtain the required temperature gradient in the pressure liner. Structural FE-analysis has been used to evaluate distribution of axial forces and interlayer axial movements to estimate the position and magnitude of relative slip between layers. The observations from both the thermal and structural FE-analyses have been basis for test set-up, procedure and selection of monitoring equipment for detecting and measuring interlayer slip.

Steady-state and transient thermal analyses have been performed in an axisymmetric thermal FE-model in Abaqus, /3/. The model is 8m long model with 0.8 m gradient zone and 1.5 m long heating and cooling zone as per the initial test (LC01-02). The 19 pipe layers are simplified to 10 thermal layers where some adjacent tape layers are merged to one homogenous layer, similar for the two pressure amour layers. The pipe layers are modelled isotropic with thermal properties (thermal conductivity, specific heat capacity and density) as defined by the pipe manufacturer. The pipe bore is assumed insulated and modelled adiabatic, i.e. no transfer of heat. Heat loss to ambient is modelled by a free convection heat transfer coefficient between the external insulation and the ambient laboratory air. Heating and cooling is applied by enforced temperatures on the outer sheath.

Various test set-up options have been analyzed in the pre-study providing insight in the surface temperatures, required energy flux and time required for heating and cooling as well as axially and radially temperature distribution in the pipe section.

Test results from a pilot test were compared to transient thermal analysis results from MARC, /4/, showing good consistency. Figure 2 shows the test and analysis results during uniform heating of the 2.6 m long test sample used in the pilot test. The red line represents the estimated temperature in the liner vs. time from analysis results, the other lines are temperature measurement in the liner along the length of the test sample. It was observed that difference between measurements and analysis results were small compared to the measured temperature variation along the length of the test sample.

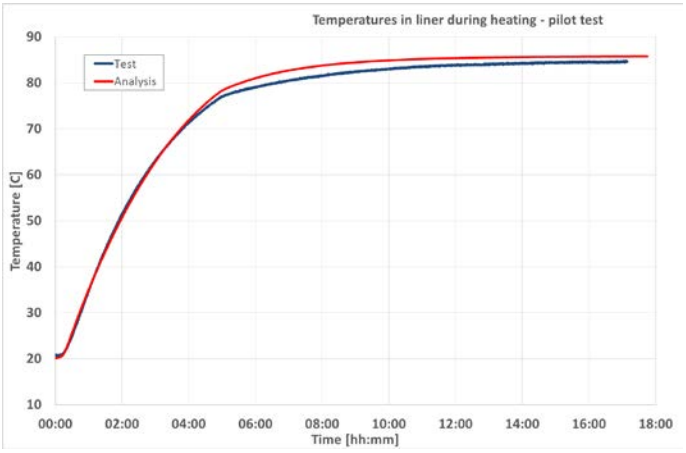

FIGURE 2. TRANSIENT ANALYSIS ESTIMATES VS. TEMPERATURE MEASUREMENTS – PILOT TEST

Similarly, analysis results from a steady state thermal analysis was compared to temperature measurements in the liner from the full-scale test, see Figure 3. The x-axis represents the axial

position along the test sample, and the y-axis the liner temperature. It is observed that the temperatures in the gradient zone are very similar between test measurements and analysis estimates.

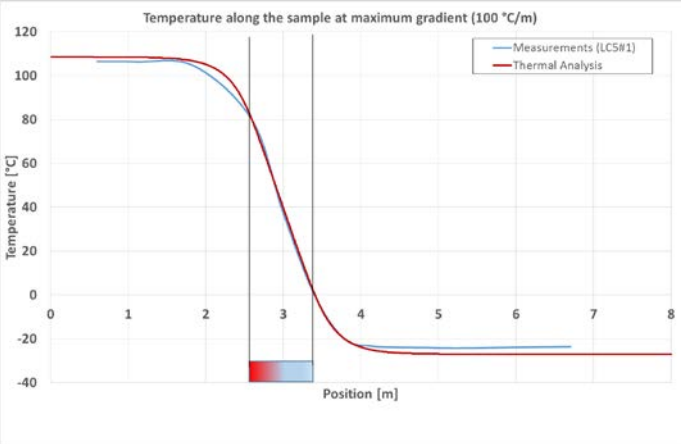

FIGURE 3. STEADY STATE TEMPERATURE ANALYSIS ESTIMATES VS. TEMPERATURES MEASUREMENTS – FULL-SCALE TEST

For the pre-test assessment of axial movement of the individual layers a detailed axisymmetric FE-model of the 8m test pipe was modelled in MARC, /4/, for the initial test (LC01-02) with 1.5m length warm and cold zones. The early understanding was that slip would occur between the pressure sheath and the pressure armour layers of the pipe driven by the temperature gradient. The analyses demonstrated that significant slip would also occur between pressure armour and tensile armour.

The structural FE analysis is performed with an axisymmetric model that includes all layers of the pipe, including insulation used during the test. An axisymmetric model is efficient considering modelling and computational time, and as a tool for studying importance of input parameters. However, relevant pipe fabrication effects such as ovality, pipe curvature, and circumferential liner thickness variation (all within acceptable tolerances) are not directly assessed. Study of these effects will require detailed 3D analyses.

In the pre-test model the individual layers are modelled as cylinders except the carcass and the pressure armour which are modelled as inter-connected rings, not helixes, see Figure 4. The tensile armour layers are modelled with correct coupling between tension, torsion and radial pressure. Only a minor geometrical coupling between pressure amour and pressure liner (creep into gap in the armour) is expected for new PVDF pipes. The friction coefficient between the pressure armour and the pressure liner include this geometrical interaction and is based on separate small-scale tests. The pre-test model include linear springs between pressure armour profiles and between carcass profiles to mimic the axial stiffness of a 3D helix. Bi-linear springs are used between pressure liner and pressure armour profiles to simulate residual contact and friction when the temperature is low and radial contact is reduced. This effect is seen in mid-scale tests and origins from fabrication inaccuracies (within tolerances).

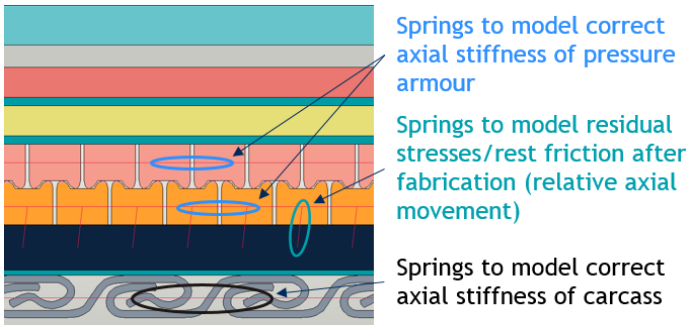

FIGURE 4. STRUCTURAL AXIS-SYMMETRIC FE MODEL (MARC, /4/)

The temperature profile as function of time from the transient thermal analysis is directly applied to the structural model as a boundary condition. The structural forces and displacements of the individual layers are determined for the temperature cycle from the test. Tension variation is applied as per procedure.

The results from the structural analysis are used to determine the temperature gradient at first slip, significant slip (5mm) and displacement at maximum temperature gradient.

The initial slip between pressure liner and pressure armour is predicted to occur at a gradient of approximately 50 °C/m. The initial slip would occur in the midpoint of the cold zone. A significant slip >5mm occur at a gradient of approximately 80 °C/m. At maximum gradient of 100 °C/m the predicted displacement of the pressure liner occurs in the middle of the gradient zone, see Figure 5. The pressure armour follows the pressure liner along the pipe except for the cold zone where contact pressure is lost and the pressure liner moves relative to the pressure armour.

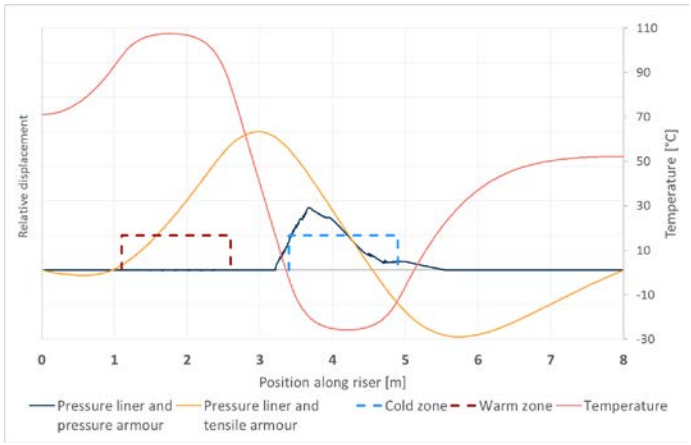

FIGURE 5. RELATIVE DISPLACEMENT BETWEEN LINER AND PRESSURE ARMOUR (DARK BLUE) FROM THE MARC (/4/) PRE-TEST MODEL. REF. TENSILE ARMOUR NOT MOVING

Observations from the thermal and structural analyses have been used as input for procedure and refinement of instrumentation positioning in cold zone and test execution.

Extended focus has been given to the position in the cold zone with expected slip between pressure liner and pressure armour.

FULL-SCALE TEST

The initial objective was to perform a test in a controlled test environment, which allows for understanding of conditions for interlayer slip induced by axial thermal gradients. If slip occurred, this should be detected and quantified. After slip was identified, the scope of the test was further expanded to study the accumulated displacements over series of thermal cycles and the corresponding level of forces experienced by the liner. Five different load cases will be referred to in the following, denoted LC01 - LC05.

In short, the test methodology include:

- A flexible pipe section with simplified end fittings
- Test frame including tension actuator and support structure and possibilities for cyclic bending of the pipe
- Thermal loading equipment (heating/cooling) including temperature sensors to control the temperature loading
- Equipment for measuring displacement of individual layers of the pipe
- Load cell for liner forces (implemented after increased test scope, LC04 - LC05)

Test setup

The test sample, test rig, test parameters and instrumentation are described in the following section.

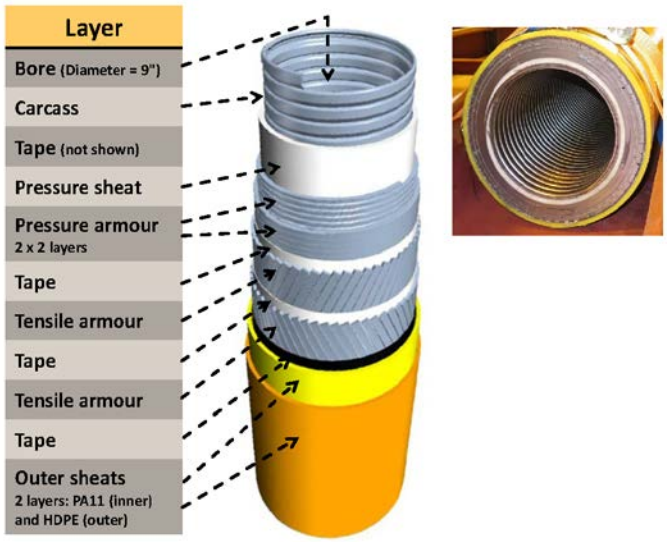

FIGURE 6. 9" FLEXIBLE PIPE, 1-LAYER PRESSURE SHEATH, TEST SAMPLE

The build-up of the pipe is shown in Figure 6. Prior to testing, the HDPE and outer tape layers were removed from the sample, keeping the PA11 sheath as the outermost layer. Simplified end fittings were installed at both ends of the specimen. Both tensile armour layers were welded to the simplified end fitting, while penetrating bolts secured the remaining layers, see Figure 7. Prior to test phase LC04 a liner force (load cell) measurement system was installed in the heated end of the sample during temperature gradient build-up, see Figure 8. The penetrating bolts were removed at this end of the pipe just after the load cell equipment were installed.

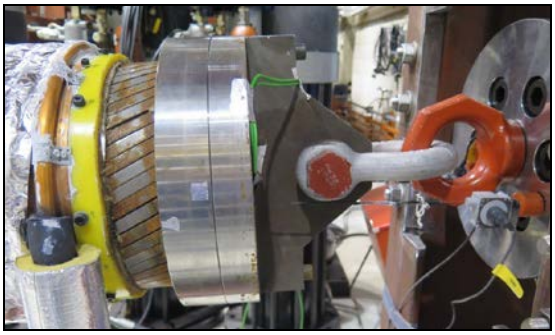

FIGURE 7. END OF TEST SAMPLE WITH SIMPLIFIED END FITTING CONNECTED TO THE TENSION ACTUATOR OF THE RIG

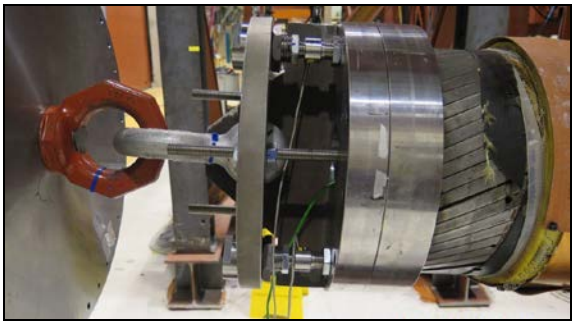

FIGURE 8. END OF TEST SAMPLE WITH SIMPLIFIED END FITTING AND LINER FORCE MEASUREMENT SYSTEM INSTALLED

FIGURE 9. TEST RIG WITH PIPE SAMPLE INSTALLED. INSULATION IS REMOVED FOR VISUALIZATION

The test rig is shown in Figure 9 with the test rig frame, a hydraulic load actuator (far right) and the test sample installed. A constant tension load of 100kN were applied during the

testing. The resulting free configuration of the pipe has a moderate sag; hence, straps are applied to achieve a straight configuration of the pipe during testing. Figure 9 to Figure 11 also shows the main components for the outside temperature loading:

- the entire pipe covered by thermal paste and copper sheets for improved thermal conductivity
- a section of the sample covered by copper coils (covered by thermal paste and aluminum foil) connected to a thermal liquid machine capable of both cooling and heating the section, seen to the right in Figure 9 and illustrated by the blue section of Figure 1
- for the remaining sections of the sample the temperature is regulated by heater mats when heating, see to the left in Figure 9 and Figure 10. An additional air-cooling and circulation system is attached when cooling below room temperature, see Figure 11.

Test Parameters

The thermal load scenarios were alternating between the following states during a test cycle, by use of illustrated equipment:

- Uniform elevated temperature (pipe in normal operation) (by equipment shown in Figure 9 and Figure 10)
- Axial thermal gradient; warm section, gradient section and cold section as per Figure 1 (cooling during shut-down) (by equipment shown in Figure 10)
- Uniform low temperature; initially room temperature, later active cooling (steady state after shut-down) (by equipment shown in Figure 11)

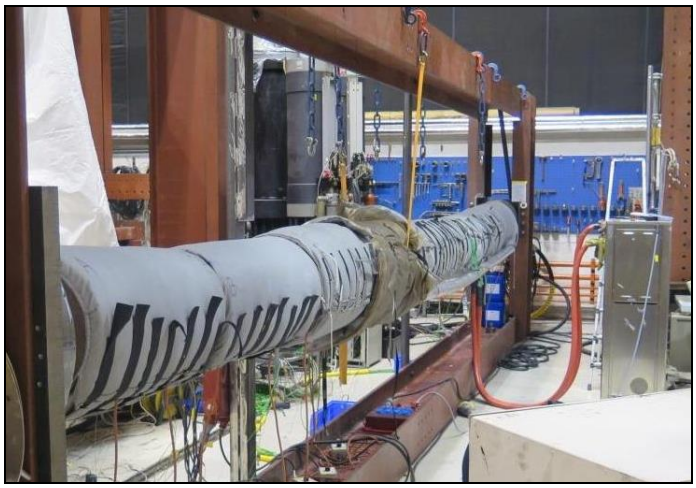

FIGURE 10. INSULATED PIPE, UNIFORM HEATING OR GRADIENT BUILD-UP

FIGURE 11. ACTIVE COOLING BY AIR CIRCULATION INSIDE SURROUNDING TUBE-SHELL.

The temperature profile in gradient state, as measured during testing for LC05 is shown in Figure 12.

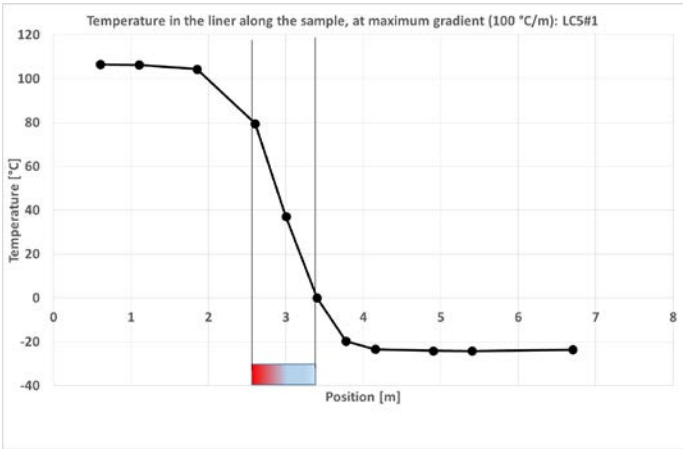

FIGURE 12. TEMPERATURE PROFILE IN LINER ALONG THE SAMPLE - AT MAXIMUM GRADIENT (LC05)

During testing, the shear forces build up under a static, straight pipe configuration, which is not very realistic for riser operational conditions. To rectify this at selected intervals during each test cycle, the pipe strapping is released, causing the pipe to sag. 10 cycles of tension variations ±50 kN is applied at 0.05Hz resulting in a combined tension-bending variation in the pipe. The strap is then re-attached; aiming at the same actuator position prior to releasing the strap.

Instrumentation

The sample was instrumented at selected locations along the pipe. Several temperature sensors were installed for each axial location, at different layers, see Figure 13. The temperature sensors were used to monitor the temperature state and control the temperature loading.

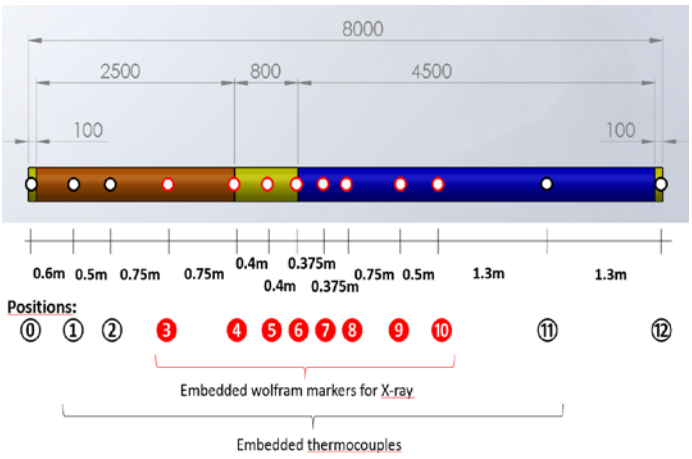

FIGURE 13. SELECTED POSITIONS ALONG THE TEST SAMPLE FOR MONITORING THE PIPE BEHAVIOUR

The key results from the test are the displacement measurements, which were also obtained at different axial locations along the pipe. During the initial stage, visual monitoring of liner displacement was performed via camera through a hole drilled down to correct level, providing only qualitative information. Three string potentiometers were installed for continuous measurements of carcass position, of which one had to be disconnected when the load cell was installed. The importance of the string potentiometers increased after sufficient confidence was established in relating the carcass and liner displacements.

The most detailed source of displacement information was based on radiography measurements conducted at different stages of the test, more frequent in the first load cases than the later ones. At several locations along the pipe, see Figure 13, a set of wolfram markers were installed into the pipe cross section, see Figure 14. A reference system for each axial position (wolfram marker) was linked to the test rig itself, ensuring the global reference to be identical for all the stages of the test.

Load Cases

Tension testing: To confirm sufficient tension capacity, the tension level was increased gradually and stepwise by 50kN to a total of 200kN. The rig and test specimen was visually inspected. No abnormalities were observed.

Preconditioning: At normal tension load (100kN), an axial uniform temperature loading to gradually obtaining 70ºC were applied. The temperature level was maintained for 18 hours. This was done to reduce possible stress gradients in the PVDF-liner.

LC01: Short temperature zones. Temperature stages: Uniform room temperature, Uniform 80ºC, Gradient zones: 40, 80 then 100ºC/m, Uniform room temperature. Axial cycling (shaking) were done at Gradient 100ºC/m and at return to room temperature.

LC02: Temperature stages identical to LC01. Axial cycling was performed at all Gradient stages and at return to room temperature.

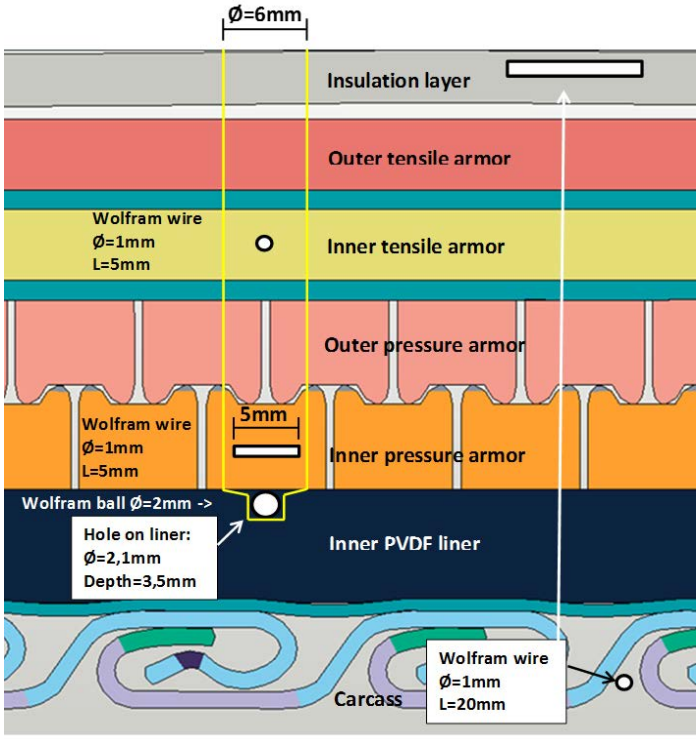

FIGURE 14. UNIQUE WOLFRAM MARKERS WERE INSERTED IN DIFFERENT LAYERS OF THE PIPE.

LC03: Length of warm/cold zones increased. Identical to LC02, except for return to +10ºC instead of room temperature.

LC04: (a total of 6 cycles): Temperature stages: Uniform room temperature, Uniform 80ºC, Gradient zone: 100ºC/m, Uniform: room temperature (3 first cycles) and 10ºC (3 last cycles). Axial cycling at gradient and return to low temperature. Note: A heating mat was active in the gradient zone during gradient build-up, shifting the position and modifying the slope and axial position of the gradient.

LC05: (a total of 7 cycles): Temperature stages: Initial Uniform room temperature. Then cycles of: uniform 80ºC, Gradient zone: 100ºC/m, Uniform: 5ºC. Axial cycling at gradient and at 5ºC.

Test Results

The governing "load" in the full-scale test is the temperatures applied to the sample in the warm and cold zones. Figure 15 shows the liner temperature in the warm and cold zones during one temperature cycle. The liner is 5°C along the liner at the start of the cycle (140 hours), before the sample is uniformly heated to 80°C. At 169 hours, additional heating is applied in the warm zone and cooling is applied in the cold zone. At 191 hours, the full gradient is achieved, and both the cold and warm zones are adjusted to 5°C again. At 215 hours,

the sample has returned to a uniform temperature of 5°C, and the cycle is completed.

Figure 16 shows the resulting temperature gradient during the same cycle. The temperature gradients gradually converge to the target of 100°C/m as the temperature in the warm and cold zones stabilizes to the defined values.

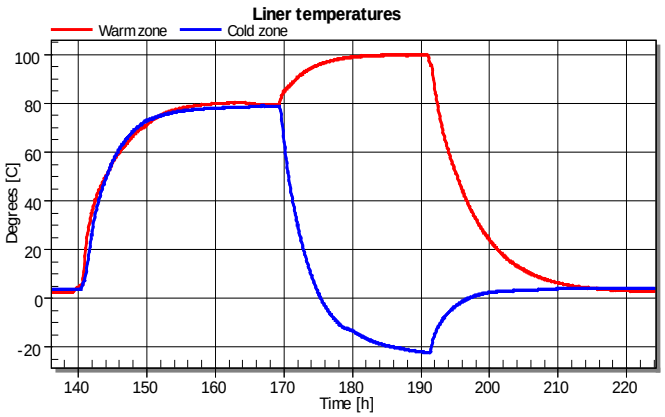

FIGURE 15. TEMPERATURE IN WARM AND COLD ZONES DURING ONE TEMPERATURE CYCLE

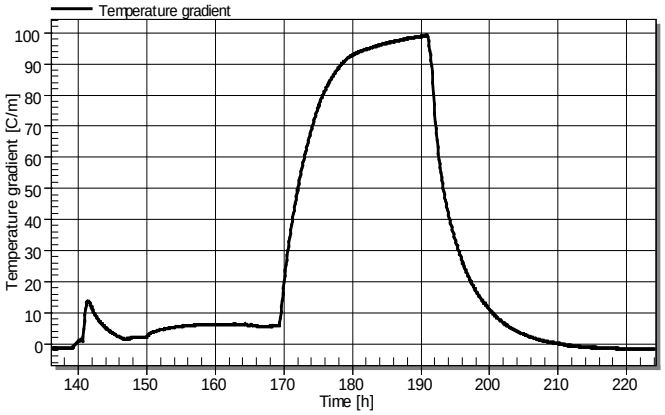

FIGURE 16. TEMPERATURE GRADIENT IN THE LINER CORRESPONDING TO FIGURE 15

The initial objective of the full-scale test was to measure if relative axial displacement (slip) occurs between the pressure armour (PA) and liner. Both instrumentation and applied temperature gradients were chosen based on the analysis results from the MARC (/4/) FE-model. In the first load case, LC01, the temperature gradient was applied in a stepwise manner, 40°C/m (pre-slip), 80°C/m (after first slip) and 100°C/m (maximum gradient).

The measurement results from LC01 of the full-scale test are presented in Figure 17. The relative displacement between the liner and pressure armour is plotted along the length of the sample for the applied gradients. At 80°C/m, a small relative displacement is observed in the cold zone, toward the gradient zone. At 100°C/m the slip has increased significantly. These findings are consistent with the finite element analysis results. The slip was confirmed by camera recordings as well.

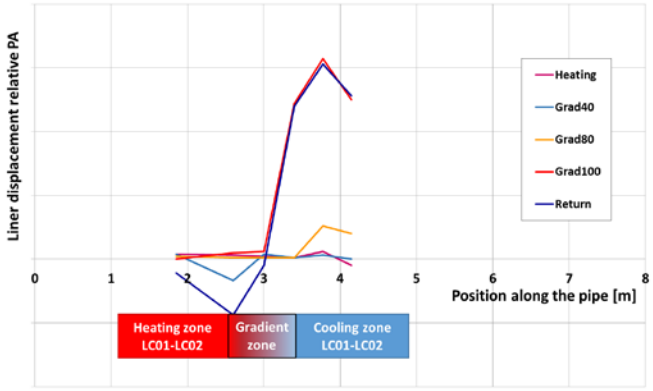

FIGURE 17. RELATIVE DISPLACEMENT BETWEEN LINER AND PRESSURE ARMOUR IN LC01.

Based on the findings in LC01, the test confirmed that slip will occur for the axial temperature gradients and test conditions applied in the laboratory.

An important observation is that the relative displacement between the liner and pressure armour does not return to zero after the sample temperature was returned to room temperature. Based on this finding, the test was continued to study if the slip would accumulate for additional temperature cycles. In this part of the test, relative displacement between all structural layers were studied; carcass, liner, pressure armour and tensile armour (TA). The relative displacement of individual layers and the tensile armour was of special interest because the tensile armour is the primary axial load-carrying member in the section.

Figure 18 shows the relative displacement between liner and tensile armour for maximum gradient (100°C/m) for LC01 - LC05. The plot shows that the magnitude of the relative displacement increases for each cycle, but the magnitude of the increase is gradually reduced. The length of the region where relative displacement is observed increases (grows) as well.

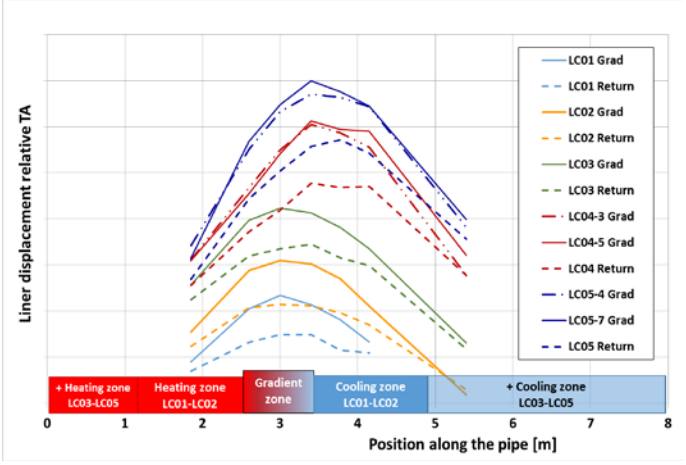

FIGURE 18. RELATIVE DISPLACEMENT BETWEEN LINER AND TENSILE ARMOUR FOR GRADIENT 100°C/M ALONG THE LENGTH OF THE SAMPLE

Similarly, the relative displacement between the pressure armour and tensile armour is plotted in Figure 19. The results show that the relative displacement between the pressure armour and tensile armour is larger than the relative displacement between the liner and the tensile armour. The position of the maximum relative displacement is in the gradient zone, towards the warm zone for the pressure armour. For the liner, the location of the maximum is in the gradient zone towards the cold zone.

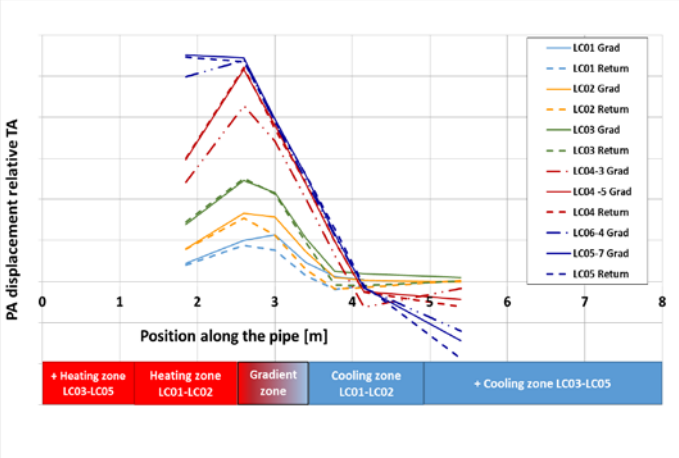

FIGURE 19. RELATIVE DISPLACEMENT BETWEEN PRESSURE ARMOUR AND TENSILE ARMOUR FOR GRADIENT 100^{O}C/M ALONG THE LENGTH OF THE SAMPLE

To achieve a better understanding of the displacement of the liner and pressure armour, plots of the incremental displacement pr. step was established. Figure 20 shows the incremental displacement for the liner and the pressure armour in position 4 (border between warm zone and gradient zone). It shows that the liner (orange) and pressure armour (blue) moves almost identically when establishing the temperature gradient. However, when returning to room temperature, the liner moves more towards the original position, but the pressure armour in a much less extent. The same is observed for LC02; the liner and pressure armour moves almost identically from uniform heating to maximum gradient, but when returning to room temperature, the liner returns towards the original position in a much larger extent than the pressure armour. These results indicate that the difference in displacement between the liner and pressure armour in position 4 occurs when cooling down the sample in this position. During heating (from 80 °C to ≈100 ° C in this region), both layers move synchronously.

Figure 21 shows the incremental displacement for the liner and pressure armour in position 8, i.e. 0.75 m into cold zone from transition between gradient zone and cold zone. From this figure, it is observed that the liner moves much more than the pressure armour when establishing the gradient (i.e. cooling this part of the sample). When returning to room temperature (warming this section), the liner and pressure armour move synchronously.

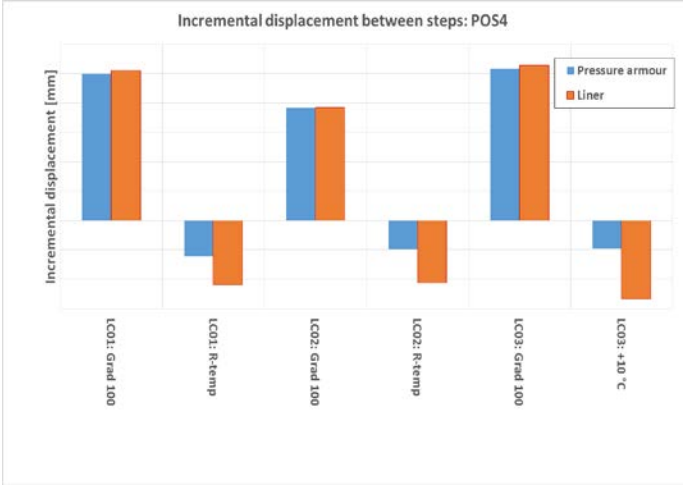

FIGURE 20. INCREMENTAL DISPLACEMENT FOR LINER AND PRESSURE ARMOUR AT POSITION 4 (TRANSITION BETWEEN WARM ZONE AND GRADIENT ZONE)

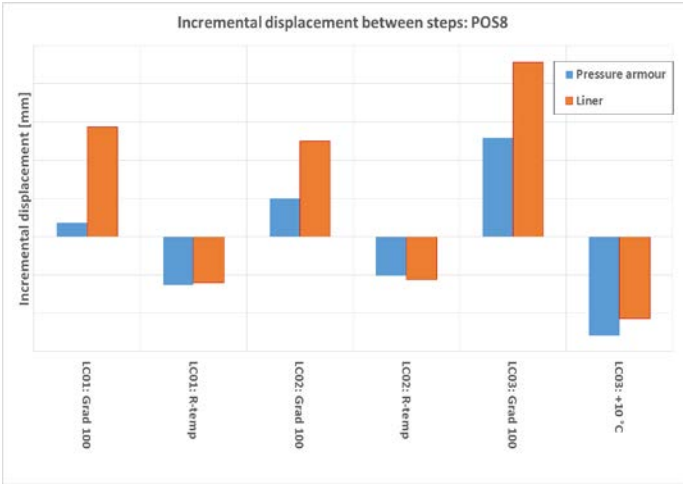

FIGURE 21. INCREMENTAL DISPLACEMENT FOR LINER AND PRESSURE ARMOUR AT POSITION 8 (0.75 M INTO COLD ZONE FROM TRANSITION BETWEEN GRADIENT ZONE AND COLD ZONE)

Figure 22 shows the relative displacement between the liner and tensile armour for each test stage (LC01-LC03) in POS3 – POS 8. This plot is interesting with respect to accumulation of displacement over repeated thermal cycles. The plot shows that the increase in displacement when applying the gradient is larger than the reduction in displacement when returning to room temperature after maximum gradient. Hence, the liner displacement is increasing over multiple thermal cycles. The corresponding plot for all load cases included is shown in Figure A2, Appendix A.

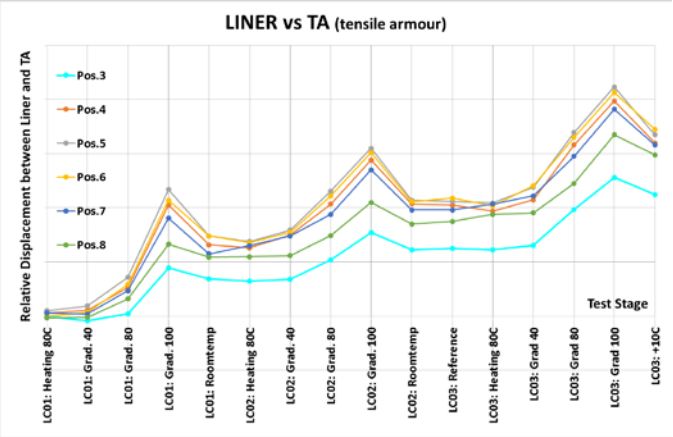

FIGURE 22: LINER DISPLACEMENT FOR EACH TEST STAGE (LC1-LC3)

Figure 23 shows the relative displacement between the pressure armour and tensile armour for each test stage (LC01-LC03) in POS3 – POS 8. The plot shows that the relative displacement increase significantly in the warm zone and gradient zone, but is relatively constant in the cold zone. The corresponding plot for all load cases included is shown in Figure A3, Appendix A.

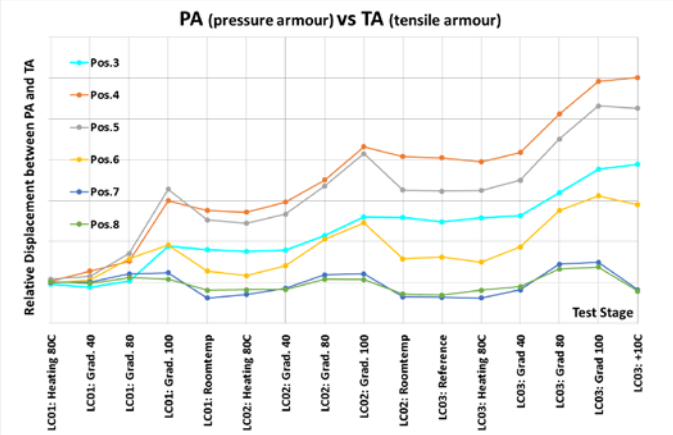

FIGURE 23: PRESSURE ARMOUR DISPLACEMENT FOR EACH TEST STAGE (LC1-LC3)

Before LC04, a system for measuring the liner force in the warm end of the pipe sample was installed. It is highlighted that force in initial cycles is not recorded and this may influence the recorded results, and discussions below. The measured force from LC04, cycle 1 to LC05, cycle 4, is shown in Figure 24.

The plot shows a compressive liner force at maximum gradient (black line), and a tensile liner force at low temperature (room temperature, 10°C or 5°C). The latter should be noted since large tensile forces in extreme cases may be critical with respect to end fitting layer termination, see API 17J 5.3.3 (2014), Ref. /1/.

The plot shows that the (compressive) force at maximum gradient is gradually reduced pr. thermal cycle. The (tensile) force when returning to low temperature, increase correspondingly in LC04, but seems to somewhat stabilize in the next thermal cycles.

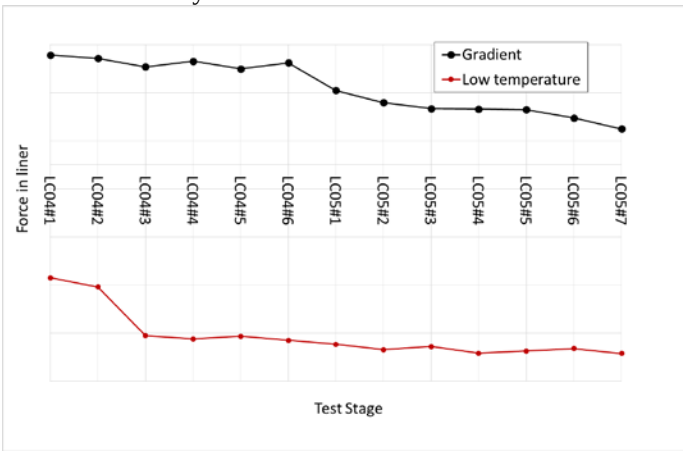

FIGURE 24. DEVELOPMENT OF LINER FORCE AT GRADIENT AND UNIFORM COLD STATE FOR LC04-05 FOR EACH TEMPERATURE CYCLE

TEST ANALYSIS

Structural FE-analysis were performed in parallel with the test execution to evaluate the load mechanisms contributing to the relative layer displacements and accumulation of these from each temperature cycle. The current working theory is that the liner is the key driver for the displacements, as the liner temperature expansion coefficient (20-80°C) is 10-20 times the coefficient for the steel layers. However, in operational pipes, the radial temperature gradients may be larger than in the test setup, and these radial gradients may impose variations in contact pressures and hence influence the friction and relative displacements.

The full structural FE-model in MARC, /4/ was refined based on learnings from the pre-test analysis, results from the tests and updated information on pipe cross section and material parameters. The latest FE-model includes updated pipe geometry to reflect key features of real pipes with pressure liner geometry interacting with both pressure armour and carcass. Pressure liner thickness and circumferential thickness variation was measured from the pipe used in the pilot test section as well as liner creep into gap to pressure armour and depth of 'knobs' into carcass from extrusion, see Figure 25. The Thermal expansion coefficient and Young's Modulus of the PVDF was updated based on testing by the pipe manufacturer and the operator Statoil. Based on all the PVDF material testing and the liner displacements recorded through the test cycles, it is evident that the material model needs to account for both visco - elastic and plastic behavior. This contrasts with previously presented FE analysis of PVDF riser end fittings during uniform cooling where a visco-elastic model with Prony series for stress relaxation gave good results compared to full and mid-scale tests, see Kristensen et.al (2014), Ref. /2/.

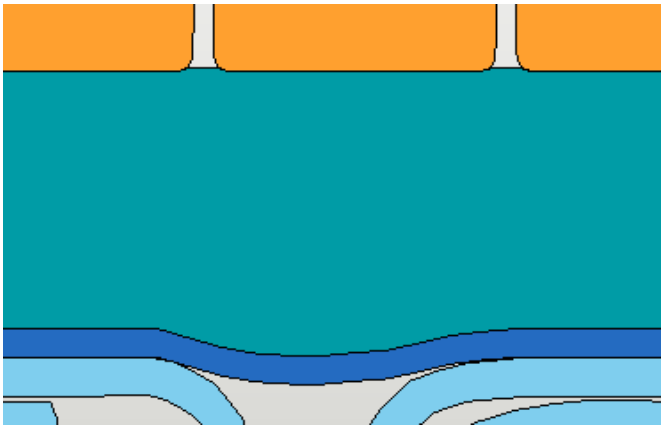

FIGURE 25. IMPROVED FE-MODEL WITH 0.1 / 1.5MM IMPRINT IN LINER FROM PRESSURE ARMOUR / CARCASS

Analyses have been run for LC01 with the improved model. The displacements for both liner and pressure armour match the results from the test well, see Figure 26. This is for both position and magnitude of the displacements when the full temperature gradient of 100°C/m is present, as well as at the temperature gradient of first slip between liner and pressure armour. During the cool down to ambient temperature the remaining displacement will be governed by magnitude of liner plastic deformation, layer contact, friction and pressure armour axial redistribution. The carcass is a “slave” of the liner deformation with only minor influence due to its own axial stiffness and internal friction as well as radial stiffness.

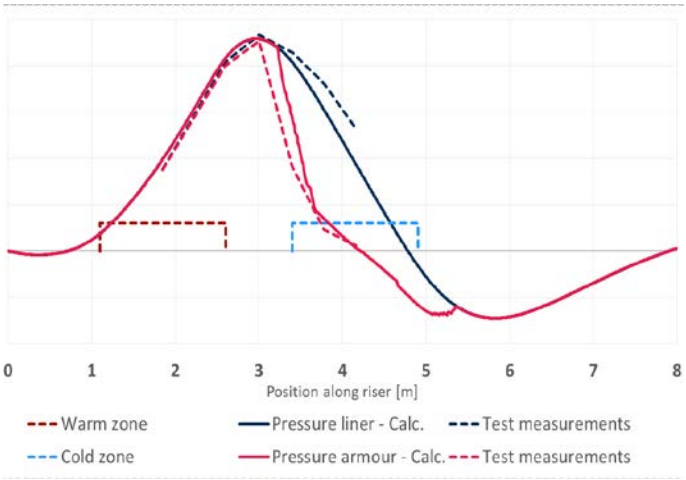

FIGURE 26. COMPARING LC01 MEASURED (DASHED) LINER (BLACK) & PRESSURE ARMOUR (RED) DISPLACEMENTS AND FE-ANALYSIS RESULTS (SOLID)

DISCUSSION / CONCLUSION

The primary purpose of the test was to study if axial temperature gradients could trigger relative displacement (slip) between the pipe layers, especially with respect to the liner and pressure armour. The test confirmed that slip will occur for the temperature gradients and test conditions applied in the laboratory. Significant slip was detected between the pressure armour, liner and the tensile armour.

Repeated temperature cycles were performed as well to study accumulation of slip/displacement. The results showed that slip continued to grow for the number of thermal cycles tested. However, the tensile force in the liner towards the simplified end fitting at the warm end seemed to stabilize towards the end of the test, most likely due to yield in the PVDF liner. The effect of yield in the PVDF liner will be further studied when the pipe is dissected after the test completion.

The presented work illustrates the importance of tests and analysis when designing and evaluating flexible pipes for high temperature applications, as well as the importance of transient condition for structural integrity of unbonded flexible pipes.

ACKNOWLEDGMENTS

The authors are grateful for the opportunity to couple Statoil’s field experiences to highly advanced full-scale lab testing and finite element analysis, with the ambition to understand critical load conditions, and improve the safety and reliability of oil & gas production.

REFERENCES

/1/ API Spec17J, "Specification of Unbonded Flexible Pipes, Fourth Edition", Section 5.3.3, (2014).

/2/ Kristensen, C.E., Muren, J., Skeie, G, Skjerve, H., Sødahl, N. (2014) "Carcass tear out load model for multi-layer pressure sheath risers". In Proceedings of the 33rd International Conference on Ocean, Offshore and Arctic Engineering, OMAE2014-24129.

/3/ Abaqus Non-Linear Finite Element Code: *https://www.3ds.com/products-services/simulia/products/abaqus/*

/4/ MARC Non-Linear Finite Element Code: *http://www.mscsoftware.com/product/marc*

ANNEX A

ADDITIONAL FIGURES

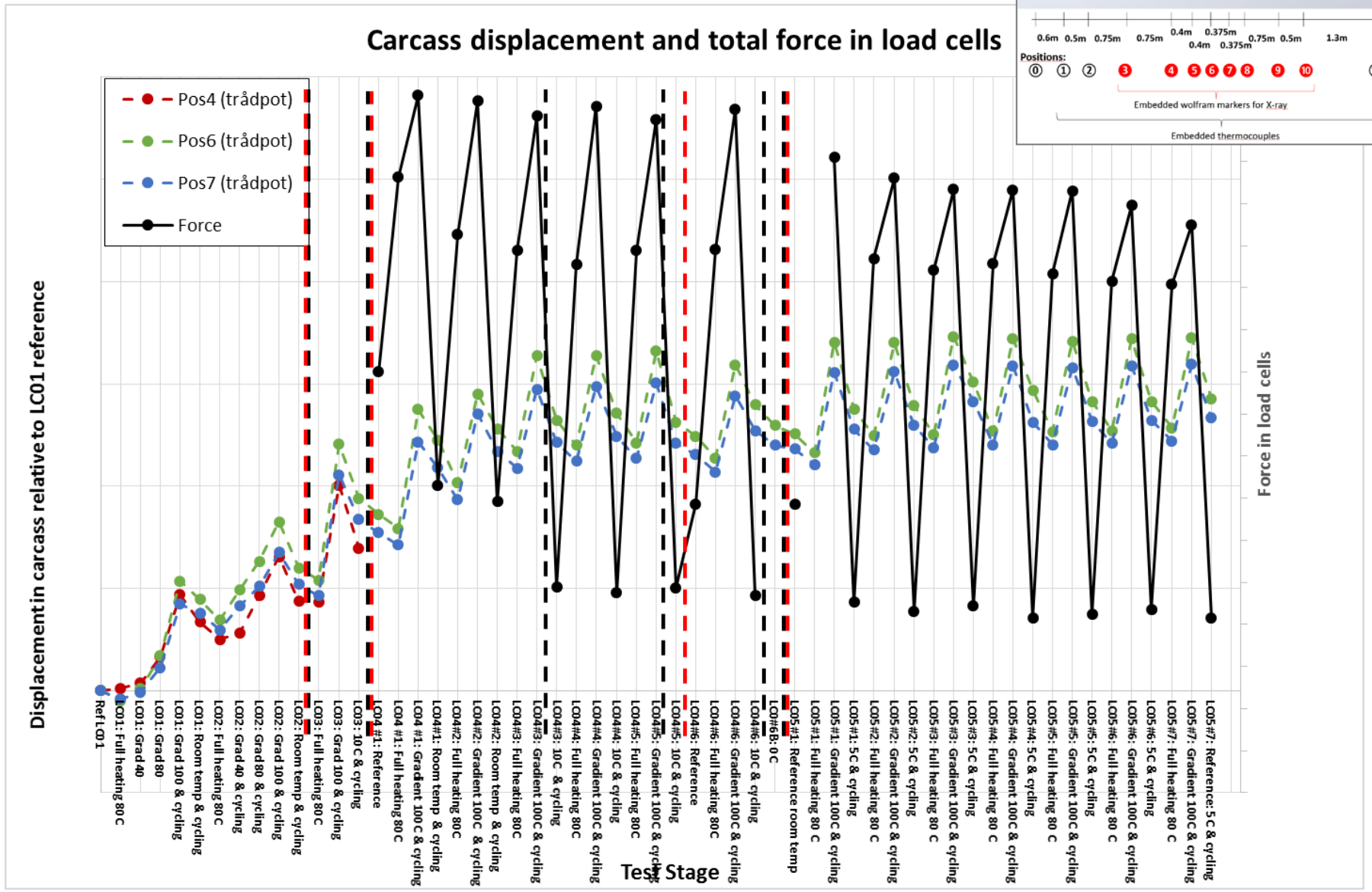

FIGURE A1 CARCASS DISPLACEMENT AND TOTAL FORCE IN LOAD CELLS FOR ALL TESTS PERFORMED

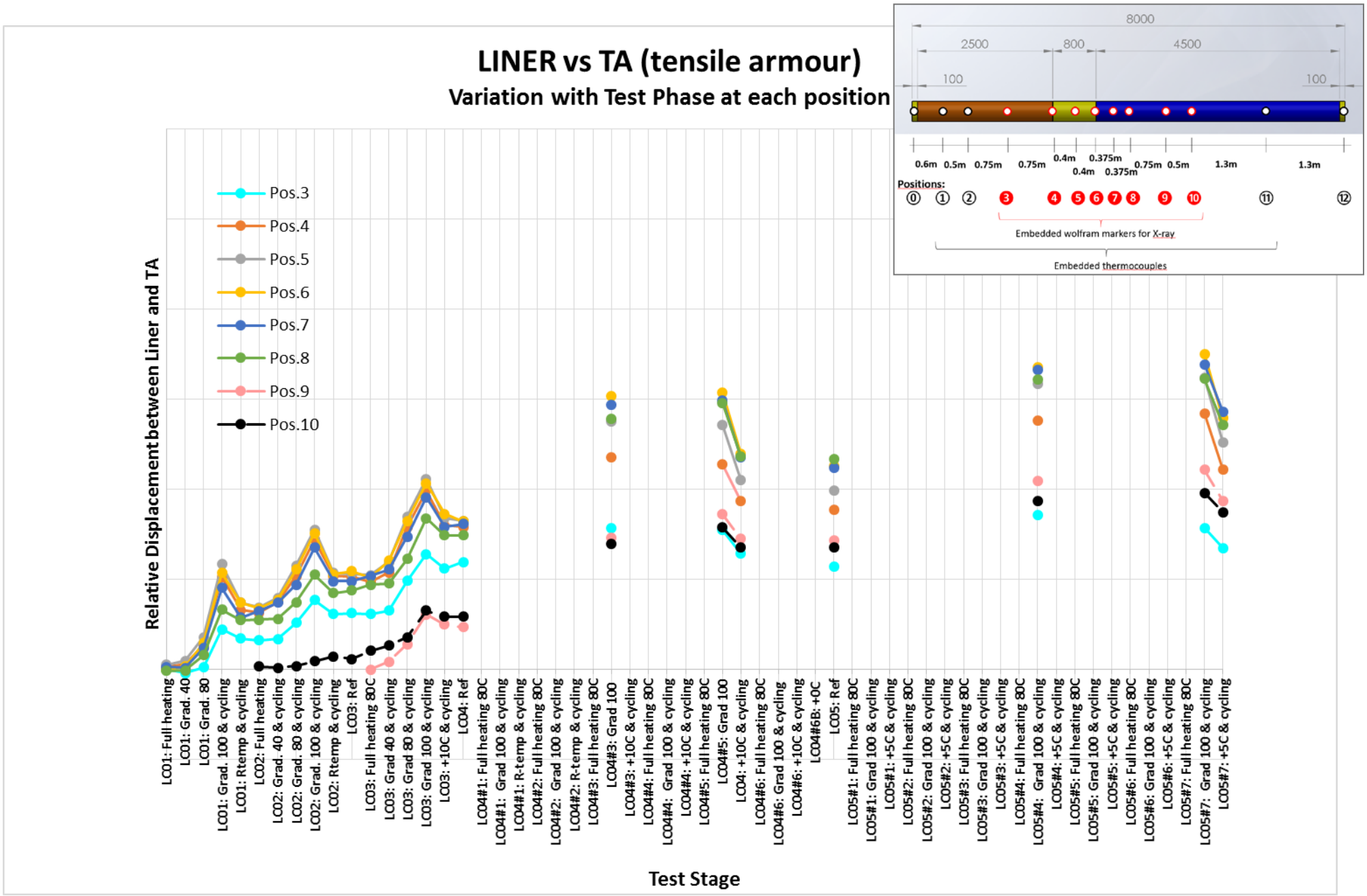

FIGURE A2 LINER DISPLACEMENT FOR ALL TESTS PERFORMED BASED ON RADIOGRAPHY

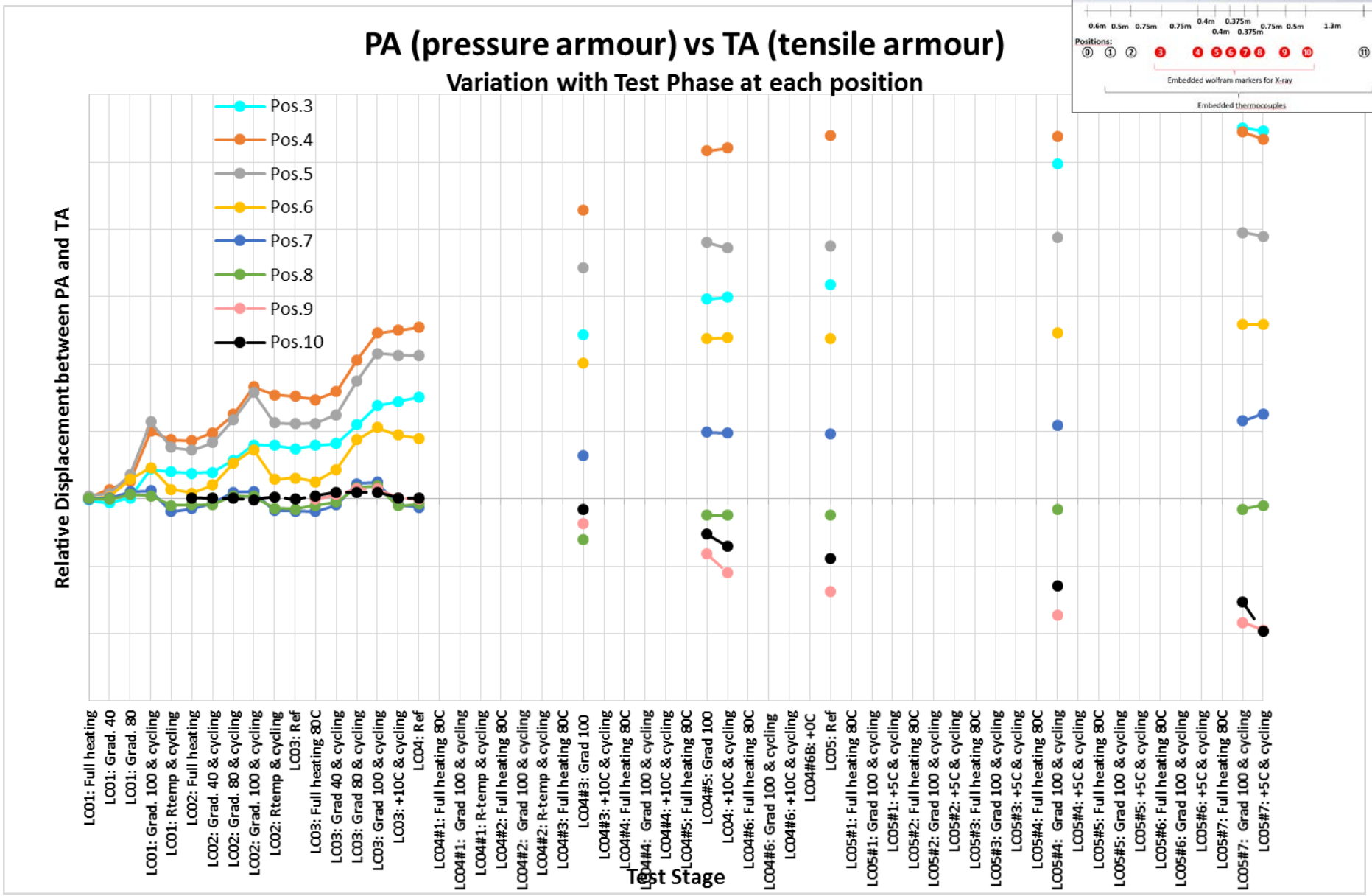

FIGURE A3 PRESSURE ARMOUR DISPLACEMENT FOR ALL TESTS PERFORMED BASED ON RADIOGRAPHY